IEEE Access
Multidisciplinary | Rapid Review | Open Access Journal

Received May 5, 2020, accepted May 27, 2020, date of publication June 2, 2020, date of current version June 11, 2020.

Digital Object Identifier 10.1109/ACCESS.2020.2999419

Poles Extraction of Underwater Targets Based on Matrix Pencil Method

XUEFEI MA[1,2,3,4], ZIQI ZHOU[2,3,4], KAIYANG LIU[2,3,4], JIARONG ZHANG[5], (Senior Member, IEEE), AND WALEED RAZA[2,3,4]

[1]College of Engineering, Tibet University, Lhasa 850000, China
[2]Acoustic Science and Technology Laboratory, Harbin Engineering University, Harbin 150001, China
[3]Key Laboratory of Marine Information Acquisition and Security, Ministry of Industry and Information Technology, Harbin Engineering University, Harbin 150001, China
[4]College of Underwater Acoustic Engineering, Harbin Engineering University, Harbin 150001, China
[5]System Engineering Innovation Center, Systems Engineering Research Institute, Beijing 100094, China

Corresponding author: Jiarong Zhang (zhangjiarong1983@163.com)

This work was supported in part by the Equipment Prophetic Field Fund under Grant 61404150301, in part by the Heilongjiang Natural Science Foundation Joint Guidance Project under Grant LH2019A006, in part by the Equipment Pre-Study Ship Heavy Industry Joint Fund under Grant 6141B042865, in part by the Underwater Information and Control Key Laboratory Open Fund under Grant 6142218061812, and in part by the Xiamen University Education Fund under Grant UAC201804.

ABSTRACT The majority of the sonic frequency bands used in active sonar detection and identification are within the resonance region of the target. The poles of target are very important characteristics of the resonance region. This paper analyzes and studies the method of extracting poles by using the matrix Pencil Method. A method which can determine the number of poles of underwater target automatically is proposed. It can average the poles that are gathered to synthesize a point as an alternative pole. Then by setting up a reasonable threshold. The poles with the higher energy in the target echo is extracted as the main pole. Aiming at the problem that the main poles of the target are missing or there are false poles in some directions, the main poles extracted from multiple directions of the target are integrated to obtain the final poles of the target. Finally, to prove the feasibility of proposed novel method echo pole extraction, the experiment was conducted in underwater spherical shell and thin rod in a silencing pool.

INDEX TERMS Matrix pencil method, orientation invariance, pole feature extraction, singularity expansion method, underwater acoustic signal processing.

I. INTRODUCTION

In the 1970s, the U.S. Air Force Weapons Laboratory first conducted a lot of research on radar poles. The purpose of the research was to improve the U.S. Air Force's combat capabilities in military aviation. An important method of pole extraction was proposed, based on the singularity expansion method which is a traditional method [1]. The singularity expansion method is one of the most important theoretical foundations in radar target detection and identification. It is pointed out that the late response of the radar echo can be fitted by a series of decaying sine wave summations, and this method can be transformed into a linear system. In addition, the characteristics of the target are closely related to the poles. These poles can be used to detect and identify radar targets.

Ideally, radar targets can be considered linear. The pole of the radar target system does not change with angle of the incident wave, form of the wave, and speed of the target's movement but is determined only by the characteristics of the target itself. This theory laid the theoretical foundation for pole detection and identification. After that, different methods for pole extraction were proposed one by one in the literature. Earlier, the Prony method failed to distinguish between early and late target echoes, because the effect of early responses on the poles was ignored [2]. Afterwards, the scientists found that the Prony method was very sensitive to noise, which would cause the accuracy of the extracted pole information, and the error generated would be large with lesser efficiency. Therefore, in practical applications, the Prony method can only be used for feature extraction and analysis of simple targets. Until 1980, Professor Brittingham *et al.* [3] tried to use the Prony method to extract the poles in the frequency domain, and the performance

The associate editor coordinating the review of this manuscript and approving it for publication was Zhaojun Li.

was improved. However, the implementation of this method was too complicated. Subsequently, a representative method that can improve performance was the KT method proposed by Kumaresan in 1982 [4]. Later, Professor Rahman introduced the singular value decomposition method into the KT method [5]. Both the KT method and the Prony method are polynomial methods. By solving higher-order equations, the poles of the target are obtained finally, but this method is very sensitive to noise when solving.

In 1974, Jain proposed the function pencil method [6], which has been applied and improved continuously. In the following decades, Hua, Rao, Mackay and Sarka *et al.* studied the idea of function pencils in depth, and proposed a generalized function pencil method, which is the matrix pencil method [7]–[9]. In 1995, Sarkar perfected the matrix pencil method [10], he studied the selection range of the pencil parameters and the method of determining the number of poles but lacked in a theoretical analysis of the parameter selection method. Matrix pencil method is a more stable algorithm than polynomial method and function pencil method. It has stronger anti-noise performance and higher calculation efficiency. It is more suitable to extract the poles of the target.

Regarding how to use the matrix pencil method to extract the pole data of the target's echo data, Song Ge proposed to use the frequency domain data obtained by FEKO software to perform pole extraction by matrix pencil method, and gave the poles of complex targets [11]. In fact, in order to obtain a large number of target poles, it is necessary to use wideband data, but sometimes such wide data is not available. In response to this problem, Janic Chauveau proposed a method for extracting target poles in narrow frequency band data. Because the number of target poles in narrow frequency band is small, and all are the main poles, the poles are extracted more easily with the higher extraction accuracy. The results show that Band data selective extraction of target poles is feasible and effective [12]. Since the poles do not change with the incident wave orientation, Sarkar uses data from multiple orientations of the target to form a correlation matrix, which improves the signal-to-noise ratio of the signal and the accuracy of the poles.

In the actual acquisition of echo data, due to the limited energy of the transmitted wave, only a limited number of poles can be excited. In the literature [13] and [14], a method based on the energy of each pole was prosed which states the corresponding attenuation factor and the size of the residues to select the dominant pole of the target, and to remove some false poles. The main pole has a greater contribution to the composition of the echo and has achieved better results for the simulation of thin wires. Reference [15] researched the poles with cavity, and [16] researched the poles of the coated medium on the surface. It was found that the resonance energy will increase with the thickness of the coating, which can increase the detection and recognition probability of the target.

Professor D. L. Moffat first tried to use the extracted poles in target recognition [17], and then proposed two methods of target recognition. One is to extract the poles from the target's scattered echo directly and compare them with the poles in the target pole library to complete the identification [18]. The other is to use the existing pole information to recover the target's late time-domain echo and store it in the recognition library, then perform a convolution operation on the measured test data echo and the data in the library. If the target data to be identified is in good agreement with the data of a target in the library, the desired output will appear after convolution, otherwise the output will not appear [19]. E-pulse method is a typical example of the second method [20]. In the laboratory environment, C.E.Baum used the E-pulse method to identify various scale models of actual targets, and obtained quite good results [21]. However, he also pointed out that the use of the E-pulse method should pay attention to some practical problems, regarding the ability of transmitted and received signals in the radar and it needs to be improved.

In China, currently a few scientific research units have researched the poles of radar or sonar targets [22]–[29]. In 1984, Zhaoben *et al.* [30] from the Institute of Acoustics of the Chinese Academy of Sciences proposed a method for classifying and identifying targets using the poles of underwater targets and conducted an underwater test on this method to identify a group of hollow cylinders with different materials, sizes, and thicknesses. It is proved that this method has better target recognition accuracy. In the 1990s, Professor Bosheng [31], [32] of Harbin Engineering University used the Prony method to extract poles from the echo signals of underwater steel balls and tried to remove false poles. In 2017, Gang and Xin [33] simulated the sound scattering field and stress distribution of a stainless steel shell. Reference [34] using a bionic dolphin to identify the cylindrical spherical shell. In the past 10 years, the team of Professor Deng Weibo of Harbin Institute of Technology has carried out research on radar pole extraction [22], [23], and performed simulation research on thin rods and solid spheres. The poles extracted by the matrix pencil method agree well with the theoretical poles. Out of the poles of complex targets (airplanes, ships, etc.).

II. PRINCIPLE DERIVATION

The system block diagram of the underwater acoustic signal processing method used in this paper is shown in Fig. 1. First, the basic principle of extracting poles by matrix pencil method is introduced, and the accurate selection of pencil parameters is discussed through simulation; The proposed method can determine the number of poles of an underwater target automatically, and then by setting a reasonable threshold, the poles with higher energy in the target echo are extracted as the main poles of the target; The main poles extracted from multiple directions of the target are integrated to obtain the final poles of the target. Finally, the experiment

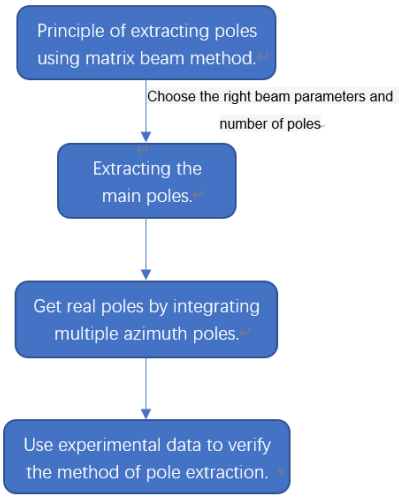

FIGURE 1. Signal processing flow chart in this article.

of echo pole extraction of underwater spherical shells and thin rods was performed in a silencing pool.

A. PRINCIPLE OF MATRIX PENCIL METHOD

With the development of the Singularity Expansion Method (SEM) theory, the research on transient electromagnetic phenomena has been promoted greatly, and the research on the transient response of sonar targets has been accelerated. Based on this, a matrix pencil method was developed. This method is used to extract the poles of the target.

The time-domain late echo model of the target impulse echo signal can be expressed as:

$$y(n) = \sum_{k=1}^{M} r_k \exp(s_k n), \quad n = 0, 1, \cdots N-1 \tag{1}$$

In the formula, N is the sampling length of the signal, and M is the number of poles of the matrix pencil method which is the number of times of exponential summation. The pole s_k and its corresponding residue r_k are the parameters to be sought. After s_k is estimated, finding the residue turns into a problem of solving linear equations.

Equation (1) can be written as:

$$y(n) = \sum_{k=1}^{M} r_k z_k^n, \quad n = 0, 1, \cdots N-1 \tag{2}$$

In the formula, $z_k = e^{s_k} = e^{(\sigma_k + j\omega_k)}$, σ_k is the attenuation factor and ω_k is the attenuation angular frequency.

Definition:

$$[Y] = \begin{bmatrix} y(0) & y(1) & \cdots & y(L) \\ y(1) & y(2) & \cdots & y(L+1) \\ y(2) & y(3) & \cdots & y(L+2) \\ \vdots & \vdots & \ddots & \vdots \\ y(N-L-1) & y(N-L) & \cdots & y(N-1) \end{bmatrix}_{(N-L)\times(L+1)} \tag{3}$$

Singular value decomposition of matrix $[Y]$,

$$[Y] = [U][\Sigma][V]^T \tag{4}$$

The matrix $[U]$ is an $(N-L)\times(N-L)$-dimensional matrix, and its column vector is the eigenvector of the matrix YY^T; The matrix $[V]$ is an $(L+1)\times(L+1)$-dimensional matrix, and its column vector is the eigenvector of the matrix Y^TY; Matrix $[\Sigma]$ is a diagonal matrix of $(N-L)\times(L+1)$ dimension. After singular value decomposition, the elements on the main diagonal of $[\Sigma]$ have been arranged in descending order from large to small. The value of the element is the square root of the eigenvalue of Y^TY, which is the singular value of $[Y]$.

When the input data is not affected by noise, the singular value decomposition of the matrix $[Y]$ will obtain M singular values greater than zero, and other singular values that are all zero. But because of the noise, the singular value of zero is disturbed and becomes a small singular value. We can suppress the influence of noise through the low-rank approximation of the matrix. By defining the following matrix:

$$\begin{aligned} [U'] &= [U(:, 1:M)] \\ [V'] &= [V(:, 1:M)] \\ [\Sigma'] &= [\Sigma(1:M, 1:M)] \\ [Y'] &= [U'][\Sigma'][V']^T \end{aligned} \tag{5}$$

The matrices $[U']$, $[V']$, and $[\Sigma']$ are part of the matrix after singular value decomposition.

Definition:

$$[Y_1'] = [U'][\Sigma'][V_1']^T \tag{6}$$

$$[Y_2'] = [U'][\Sigma'][V_2']^T \tag{7}$$

In the formula, $[V_1']$ and $[V_2']$ are obtained by deleting the last and first rows of $[V']$, Take the generalized inverse matrix $[Y_2']^+$ of matrix $[Y_2']$, then find the eigenvalues of matrix $[Y_2']^+[Y_1']$ to get z_i, and then log the z_i to get the poles of the signal.

Since the selection of the pencil parameter L has a great influence on the performance of the algorithm, the optimal value of the pencil parameter will be determined by simulation. In order to reach a more general conclusion, the target of the simulation is two kinds of objects with large differences in shape, such as a spherical shell and a thin rod.

Spherical shell parameters: radius is 0.25m, thickness is 0.005m. Simulate the frequency band covering the target resonance zone, that is, the interval frequency point in the range of 25-10000Hz. Under the condition of no noise, the sound field scattering sound pressure data with a length of 400 is obtained. Then perform inverse Fourier transform on the data to obtain the time-domain transient response echo data of the target, as shown in Fig. 2, and the time-domain sampling frequency is 20000Hz.

Select the 69th to 399th points of the time-domain transient response as the target time-domain late response, which is the length N and equals to 331 points in total. Literature [35] pointed out that when the pencil parameter is

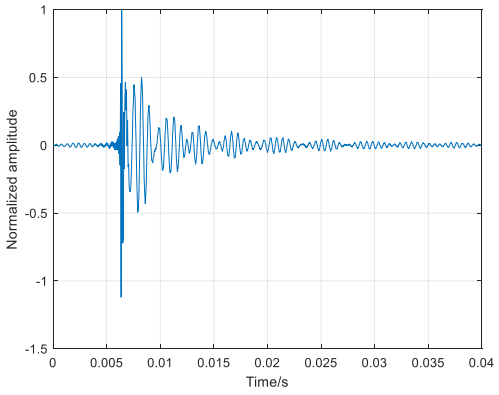

FIGURE 2. Transient echo of the underwater spherical shell.

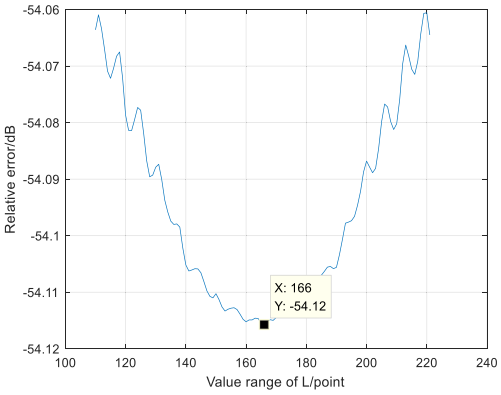

FIGURE 3. Variation of reconstructed echo error with pencil parameters.

$N/3 \leq L \leq N * 2/3$, the extraction effect of the pole is better, so the range of the pencil parameter in the simulation is 110-221, and the pole and the corresponding residue are extracted by the matrix pencil method. $y_{rec}(k)$ represents the time-domain data fitted to the extracted poles and residues, and $y_{cal}(k)$ represents the original time-domain data.

Definition:

$$err = \sum_{k=1}^{N} (y_{rec}(k) - y_{cal}(k))^2 \tag{8}$$

The optimal value of the pencil parameters is determined by *err*.

Fig. 3 is the variation curve of the echo error reconstructed by the extracted poles and residues of the underwater spherical shell with the pencil parameters of the matrix pencil method. It can be seen from Fig. 3 that when $140 < L < 180$, where the length N is 331, the fitting effect is better, and when $L = N/2 \approx 166$, the fitting effect is the best, and the accuracy of pole extraction is the highest.

The parameters of the thin rod are: length is 1m, diameter is 0.01m, that is, the ratio of length to diameter is 100. Simulation of frequency bands covering the target resonance zone is at intervals of 20-8000Hz. The time-domain transient response echo data of the target is shown in Fig. 4. The time-domain sampling frequency is 16000 Hz.

Select the 54th to 399th points of the time-domain transient response as the target time-domain late response and the length N is 346 points in total. The range of the pencil parameters is selected between 115-231, and the poles and corresponding residues are extracted by the matrix pencil method. Still use (8) to determine the optimal value of the pencil parameters.

Fig. 5 is the variation curve of the echo error reconstructed by the extracted poles and residues of the underwater thin rod with the pencil parameters of the matrix pencil method. It can be seen from Fig. 5 that when $128 < L < 220$, where the length N is 331, the fitting effect is better, and when $L = N/2 = 173$, the fitting effect is the best, and the accuracy of pole extraction is the highest.

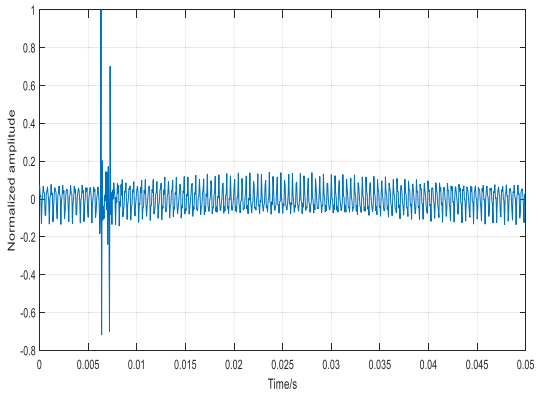

FIGURE 4. Transient echo of the underwater thin rod.

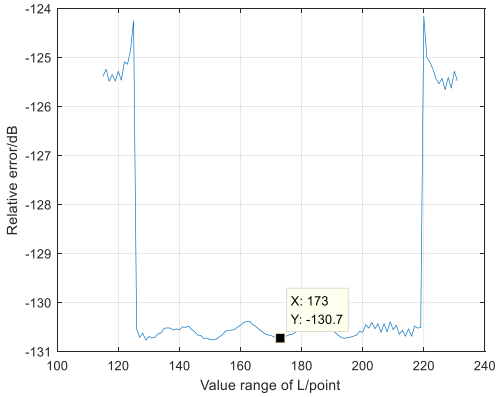

FIGURE 5. Variation of reconstructed echo error with pencil parameters.

From the above simulation results and numerical analysis, it can be concluded that when using the matrix pencil method, it is appropriate to select the pencil parameter as half of the input time domain signal length, that is which is $L = N/2$.

B. DETERMINE THE NUMBER OF EXTRACTED POLES

At present, the problem of pole extraction of underwater targets is very rare in the literature at home and abroad. The problem of pole extraction of targets in the radar field is very common. In order to facilitate comparison and analysis,

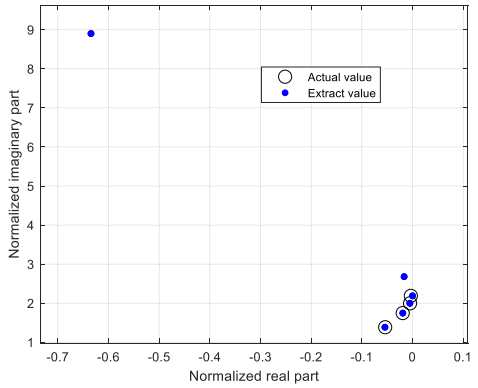

FIGURE 6. Pole distribution with 6 pairs of poles.

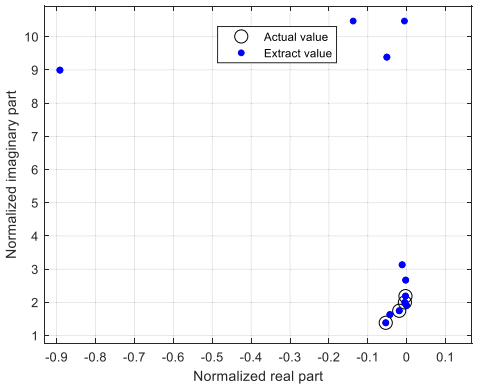

FIGURE 7. Pole distribution with 12 pairs of poles.

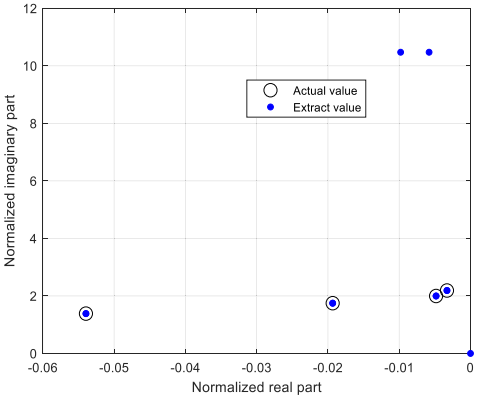

FIGURE 8. The number of poles in the spherical shell after 5-23 pairs integration.

the actual values in the target pole map of this article are the final estimated values of the real poles obtained by the method described in Section *C* and *D*.

Extract the poles of the target from its late time domain response, provided that the number of poles is known. Too large or too small number of poles will affect the extraction accuracy. If the number of poles is set too large, although the real poles will all be extracted, it will also bring many false poles; If the number of poles is set too small, there will be a large deviation between the extracted poles and the real poles, and some of the real poles will be missed.

From theoretical analysis and many simulations results obtained in matrix pencil method, it can be concluded that the extracted values of the target poles will gather around the real poles according to the number of preset poles, and the simulated false poles will be distributed in the complex plane randomly and will not cluster. This article uses this property to propose a method which can determine the number of poles of underwater target automatically. The specific measure is to average the poles that are gathered to synthesize a point as an alternative pole. This will not only determine the number of target poles, make the poles more accurate, but also eliminate false poles.

In summary, the steps proposed in this article to determine the number of target poles are as follows:

1) When the number of poles is set $M_{\min}$ to $M_{\max}$, Use the pole extraction method to extract the pole value of the target at the corresponding number of poles and store it in the matrix. Generally, $M_{\min} \geq 10$, $M_{\max} \leq N/6$, N is the length of the input data.
2) When $M = M_{\max}$, the extracted pole is $S_i^{(M_{\max})}$. Define $S_i' = S_i^{(M_{\max})}$, $i = 1, 2, \ldots, M_{\max}$. S_i' is the possible real pole, and the next cycle begins.
3) For the poles saved in step (1), use the aggregation properties of the poles to perform relevant calculations. After determining the pole $S_j^{(M)}$ at $M = M_{\max} - 1$, the error $e_{ij} = S_i' - S_j^{(M)}$ is calculated for the poles obtained from the number of adjacent poles. If $\left|real(e_{ij})\right| < \Delta\sigma$ and $\left|imag(e_{ij})\right| < \Delta\omega$ ($\Delta\sigma$ takes one-half of the smallest distance difference between the real parts of all the poles in S_i', where the distances are all greater than zero; $\Delta\omega$ takes one half of the smallest distance difference between the imaginary parts of all the poles in S_i'), $S_j^{(M)}$ is considered to be around S_i'. Use a one-dimensional matrix to store the poles S_{ij} in S_i' that meet the error threshold as alternative poles. Update parameter $S_i' = S_j^{(M)}$, $S_j^{(M)} = M_{\max} - 2$.
4) Repeat step (3) for the poles extracted by the number of poles $M_{\max} - 2$ to $M_{\min}$ to obtain a matrix of possible poles S_{ij} of the target. The number of poles in the statistics matrix S_{ij} is *num*.
5) Extract the imaginary parts of the poles in the matrix and arrange them in descending order. Set the initial value of *Numberpole* to 1, indicating the number of poles gathered near a certain pole. Then loop the sorted pole matrix: calculate the error $err_{ij} = S_i - S_j$ from the beginning pole $S_{ij}(1)$ to the last $S_{ij}(num)$ pairwise adjacent. If err_{ij} satisfies $\left|real(err_{ij})\right| < \Delta S_\sigma$ and $\left|imag(err_{ij})\right| < \Delta S_\omega$ (Generally, $\Delta S_\sigma = 0.001 * a/c$, $\Delta S_\omega = 0.001 * a/c$, a is half of the radius or length of the target, and c is the speed of sound in water), then S_i is near S_j, so $Numberpole = Numberpole + 1$; If err_{ij} does not satisfy the threshold, determine whether the parameter *Numberpole* is greater than the threshold

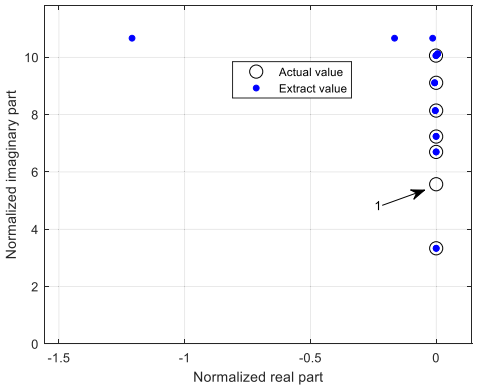

FIGURE 9. Pole distribution with 9 pairs of poles.

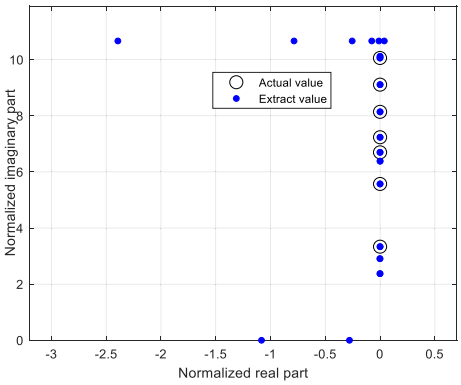

FIGURE 10. Pole distribution with 17 pairs of poles.

(General threshold is $\zeta = 0.5 * (M_{\max} - M_{\min})$. If it is, then consider S_i to be the required pole and average the *Numberpole* poles that are gathered, otherwise remove pole S_i as a false pole and set *Numberpole* to 1, and continue the cycle until the cycle ends.

To prove the feasibility and effectiveness of the proposed method, this article simulates the extraction of poles on those as mentioned earlier underwater spherical shells and underwater thin rods. The simulation conditions are similar to the simulation of selecting the pencil parameters. The only difference is that the simulated variables are changed from the pencil parameters to the number of poles, and the pencil parameters are fixed to half the length of the input time domain signal. These poles appear in pairs as conjugates, so the poles given in the figure are all poles whose imaginary part is not less than zero.

Pole extraction simulation of the late time domain response data of the underwater spherical shell is within the range of the number of pole pairs 5-23. Then divide the obtained extreme values by c/a for normalization (c is the speed of sound in water and a is the radius of the spherical shell).

Fig. 6 is the pole distribution of the target when the number of poles is 6 pairs.

Fig. 7 is the pole distribution of the target when the number of poles is 12 pairs.

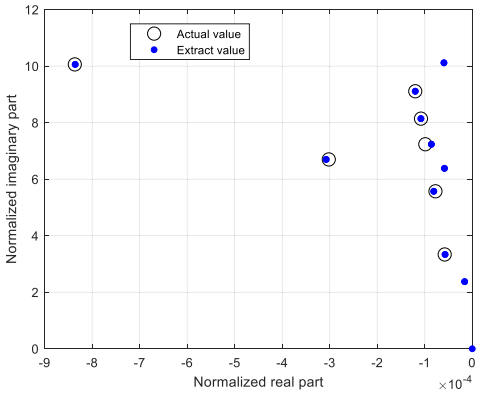

FIGURE 11. The number of poles in thin rod after 8-28 pairs integration.

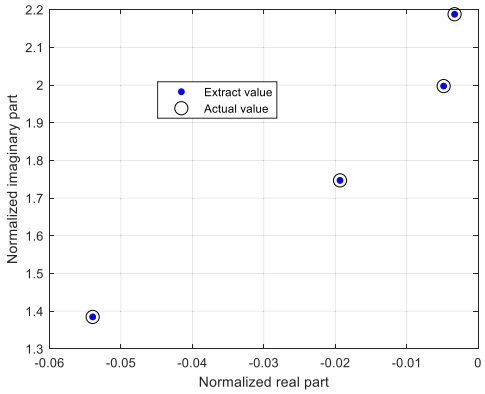

FIGURE 12. The main pole of the underwater spherical shell.

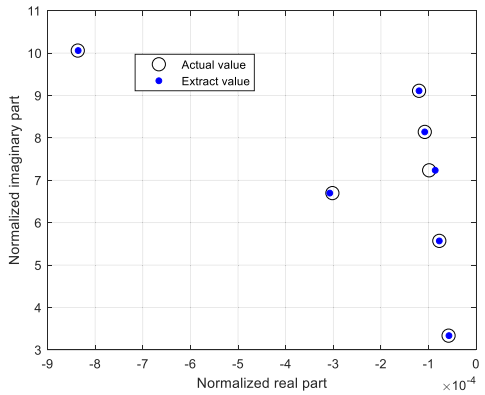

FIGURE 13. The main pole of the underwater thin rod.

From these two pictures, it is clear that the actual poles of the spherical shell have been extracted, but as the number of poles set increases, the false poles are distributed in the diagram randomly. Fig. 8 is a pole figure obtained after the integration of the above pole number determination step under the condition that the number of poles is 5-23 pairs. As a result, 7 pairs of target poles were retained, the number of false poles was reduced, and the actual poles were extracted accurately. Although there are still a small number of pseudo

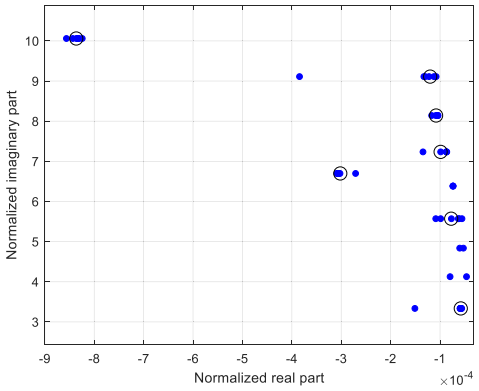

FIGURE 14. General map of the main poles extracted from the 9 positions of the underwater thin rod.

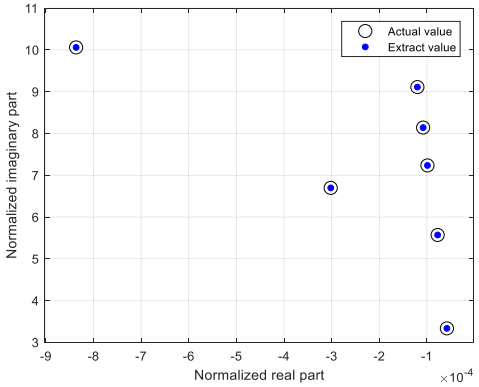

FIGURE 15. Pole distribution after integration of multi-azimuth poles.

poles, we can delete them by selecting the target main pole later.

Next, extract the extreme points of the reverse sound scattering data of the underwater thin rod when the incident wave azimuth is 20 degrees, and the number of poles ranges from 8-28 pairs. Divide the obtained extreme values by $\pi c/l$ for normalization (c is the speed of sound in water and l is the length of the thin rod). Fig. 9 is the pole value of the target when the number of poles is 9 pairs. One of the actual poles with a quite small remaining number has not been extracted, and a few poles have a large extraction error.

Fig. 10 is the pole value of the target when the number of poles is 17 pairs. All of the actual poles of the target have been extracted.

Fig. 11 is a pole figure obtained after the integration of the above pole number determination step under the condition that the number of poles is 8-28 pairs. As a result, 11 pairs of target poles were retained, the number of false poles was reduced, and the actual poles were extracted accurately.

The above simulation results and numerical analysis confirm the effectiveness of the method for determining the number of poles. Because the extracted poles are averaged, the anti-noise performance is enhanced, and the resulting poles are more accurate, and some false poles can be eliminated. Although there are still a small number of pseudo

TABLE 1. Data when selecting the main pole of an underwater spherical shell.

Num	Pole	Residue	Relative energy
1	-0.0000+0.0000i	$2.3870*10^{-7}$ - $3.4955*10^{-8}$i	0.0001
2	-0.0540+1.3846i	$1.8833*10^{-4}$ + $1.3868*10^{-5}$i	1.0000
3	-0.0193+1.7469i	$-6.8119*10^{-5}$ + $5.0743*10^{-6}$i	0.4230
4	-0.0049+1.9971i	$1.2094*10^{-5}$ + $3.0148*10^{-6}$i	0.0660
5	-0.0037+2.1886i	$-1.2301*10^{-6}$ + $1.9733*10^{-7}$i	0.0067
6	-0.0058+10.472i	$4.8712*10^{-6}$ - $1.7793*10^{-20}$i	0.0188
7	-0.0981+10.472i	$9.5959*10^{-6}$ + $2.7676*10^{-19}$i	0.0370

poles, we can delete them by selecting the main pole of the target and integrating the multi-azimuth poles, and we get the actual poles finally.

C. TARGET'S MAIN POLE SELECTION

In the actual data acquisition, the problem of limited frequency range cannot be avoided. Under the limitation of this situation, all the poles of the target cannot be excited. Therefore, the target can only be excited from the main pole selectively, which is a pole with a larger energy extracted from the target echo. This article uses the following steps to select the main pole of the target:

1) The poles are either real numbers or appear as conjugate symmetric complex numbers. Therefore, only the poles whose attenuation factor is less than zero and whose attenuation angular frequency is greater than zero ($\sigma_i < 0, w_i > 0$) can be selected.
2) When the scattered sound pressure response frequency is $f_{\min} - f_{\max}$, its pole imaginary part attenuation angle frequency should be $2\pi f_{\min} < w_i < 2\pi f_{\max}$.
3) By calculating the residues of the poles obtained in steps (1) and (2), the relative energy expression is obtained as $E_i = |R_i| / |\sigma_i|$. R_i and σ_i are the residue and attenuation factor of the i-th pole.
4) By calculating $E_i = E_i / \max(E_i)$, and keeping the pole value corresponding to the threshold p (reference [23], 0.001 is taken generally) as the main pole.

Select the main pole corresponding to the pole of the underwater spherical shell and the underwater thin rod. According to the calculation of the main pole selection steps, the data of the pole, residue and relative energy of the main pole which is selected by the underwater spherical shell are shown in Table 1.

Sort the data in the table by the imaginary part of the pole. Extreme values are normalized by c/a. The table only lists the poles whose pole imaginary part is not less than zero and the corresponding residues. Among them, the poles with the serial numbers "1", "6", and "7" whose imaginary parts are not in the range of $f_{\min} - f_{\max}$ are removed as false poles. Obviously, the total energy of the removed poles is very small.

After removing the false poles, the main pole of the underwater spherical shell can be obtained as shown in Fig. 12.

TABLE 2. Data when selecting the main pole of the underwater thin rod.

Num	Pole	Residue	Relative energy
1	-0.0000*10^{-5} + 0.0000i	8.5167*10^{-12} + 2.2667*10^{-19}i	0.0000
2	-1.6071*10^{-5} + 2.3740i	1.5218*10^{-10} - 4.5773*10^{-10}i	0.0001
3	-5.8000*10^{-5} + 3.3358i	1.4044*10^{-7} - 1.2794*10^{-7}i	0.2383
4	-7.7456*10^{-5}+ 5.5711i	2.1312*10^{-9} - 2.9390*10^{-9}i	0.0060
5	-5.8525*10^{-5} + 6.3834	2.6383*10^{-11} - 1.9182*10^{-10}i	0.0003
6	-3.0191*10^{-4} + 6.6980i	5.0642*10^{-7} - 3.0010*10^{-7}i	0.7385
7	-9.8841*10^{-5} + 7.2351i	-5.5983*10^{-8} - 4.4024*10^{-8}i	0.1177
8	-1.0797*10^{-4} + 8.1413i	1.5791*10^{-9} + 8.7770*10^{-10}i	0.0023
9	-1.2001*10^{-4} + 9.1105i	4.3444*10^{-10} + 2.1886*10^{-9}i	0.0028
10	-8.3551*10^{-5} + 10.0598i	1.7883*10^{-7} + 7.7683*10^{-7}i	1.0000
11	-5.9633*10^{-5} + 10.1164i	-4.0045*10^{-10} - 2.4663*10^{-10}i	0.0008

Now, the main poles are selected, all false poles are eliminated. This proves that the main pole contains the main energy of the target's late response echo.

Table 2 shows the data of the pole, residue and relative energy when the main pole is selected by underwater thin rod.

The data is sorted by the imaginary part of the poles in the table, and the poles are normalized by $\pi c/l$. The table only lists the poles whose pole imaginary part is not less than zero and the corresponding residues. The pole with the serial numbers "1" whose imaginary parts is not in the range of $f_{\min} - f_{\max}$ is removed as false pole. The poles numbered "2", "5", and "11" were removed because the relative energy was too small. Obviously, the total energy of the removed poles is very small, which is not enough to affect the structure of the late echo in the target time domain.

After removing the false poles, the main pole diagram of the underwater thin rod can be obtained, as shown in Fig. 13.

All the false poles have been eliminated from the poles after the main pole selection step as shown in the above figure, and only the poles that coincide with the actual poles have been retained.

D. TARGET MULTI-FACETED POLE INTEGRATION TO DETERMINE ACTUAL POLES

The location of the poles of an underwater target depends on the characteristics of the target (such as the size, shape, and material of the target), and has nothing to do with the orientation of the incident wave. It has orientation invariance and good stability. Next, the target multi-azimuth poles are integrated. The specific steps are:

1) Calculate the main poles of each azimuth target by simulation and store them in the matrix to obtain a matrix of possible poles S_{ij} of the target. The number of poles in the S_{ij} matrix is num.
2) Sort the poles in the matrix according to the size of the imaginary part. Set the initial value of *Numberpole* to 1, *Numberpole* represents the number of poles gathered around the suspected real pole. Then loop through the sorted poles: Calculate the error $err_{ij} = S_i - S_j$ from the initial pole $S_{ij}(1)$ to the last $S_{ij}(num)$.If err_{ij} satisfies $\left|real(err_{ij})\right| < \Delta S_\sigma$ and $\left|imag(err_{ij})\right| < \Delta S_\omega$, (Under normal circumstances, $\Delta S_\sigma = 0.001 * a/c$, $\Delta S_\omega = 0.001 * a/c$, a is the radius or length of the target, c is the speed of sound in water), Then S_i is near S_j, make $Numberpole = Numberpole + 1$. If err_{ij} does not meet the threshold, determine whether there is $Numberpole > \zeta$. (Literature [23] pointed out that the general threshold is $\zeta = 0.6 * n$, and n is the number of directions involved in the pole integration process.) If it is established, the pole S_i is regarded as the real pole of the target, and average the *Numberpole* poles gathered together. Otherwise, it is regarded as a pseudo pole. Reset the value of *Numberpole* to 1 and repeat the calculation until the end of the cycle.

In order to verify the feasibility of the method. Integrate the main poles of the nine azimuths of the underwater thin rod. Nine orientations refer to 0 to 80 degrees, with step intervals of 10 degrees, 0 degrees for extraction from the thin rod front and horizontal directions, and 90 degrees for extraction from the ends of the thin rod.

Fig. 14 shows the positions of the main poles extracted from the 9 positions of the underwater thin rod on the same picture. There are many poles around the actual poles of the target, but there are also some false poles scattered outside the actual poles randomly.

Fig. 15 illustrates that the main poles in the nine azimuths are comprehensively processed through the above-mentioned multi-azimuth integration step, and the pseudo poles are also removed, and finally the actual poles of the target are obtained.

III. EXPERIMENTAL DATA PROCESSING

In this section, the target echo data collected experimentally in the silencing pool are extracted and analyzed to verify the correctness of the novel proposed method.

In order to obtain the time-domain late echo data of inverse acoustic scattering of real underwater targets, the target echo experiments were performed in the silencing pool of the Harbin Engineering University experimental building. The experimental layout is shown in Fig. 16. The target and the sonar system with the receiver and the transmitter are at the same vertical depth of 5m, which is 1/2 of the pool. The distance from the target center to the transducer is approximately 6.5m. The sampling frequency of the collector in the experiment is 48000Hz. A standard non-directional signal generator generates LFM signals. After being amplified by a power amplifier, it is emitted and excites the target to generate a backscattered echo. A standard hydrophone collects the

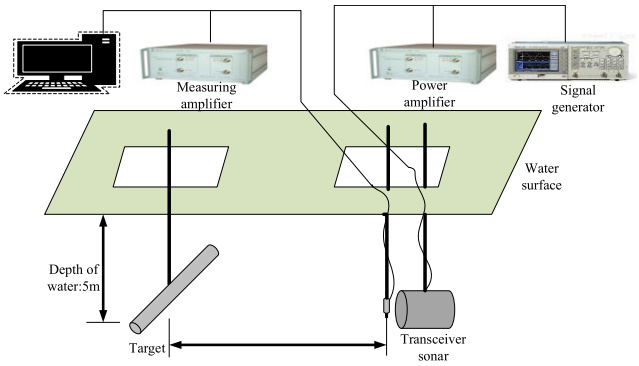

FIGURE 16. Experimental equipment layout.

FIGURE 17. Hollow steel spherical shell and solid steel rod for experimental purposes.

FIGURE 18. Finite element method solution steps.

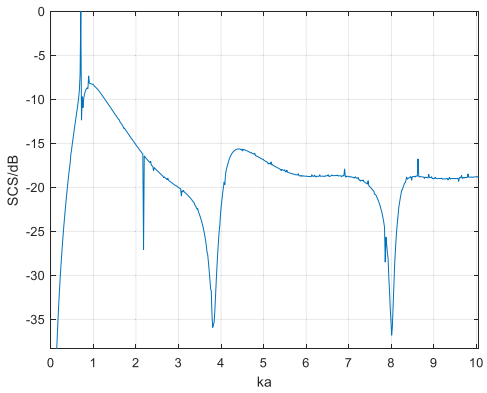

FIGURE 19. Sonar scattering cross section of the underwater spherical shell.

signal, and it passes through a measurement amplifier, and finally saved by a computer.

The target of the experimental measurement is shown in Fig. 17. The steel ball shell has a radius of 0.1m and a thickness of 0.3mm. The solid steel rod has a length of 0.7m and a radius of 17.5mm.

In order to predict the characteristics of the scattered sound field echo of an underwater target. First, we use COMSOL software to calculate the target's scattering cross section and

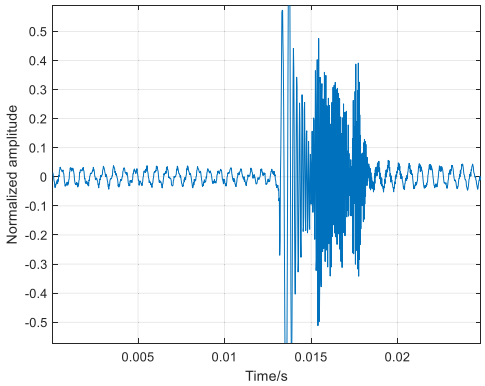

FIGURE 20. Time domain echo response of the underwater spherical shell.

time domain response of the same size and extract the actual poles, then extract the poles of the target through experimental data. Finally, we compared and analyzed the two data for further signal processing.

The steps of applying finite element solution in this paper are shown in Fig. 18. The specific steps are:

1) Define the geometric model. Select the geometric model that matches the target and define the model parameters according to the actual size of the target.
2) Choose material. The material selected is alloy steel. The specific parameters are as follows: Young's modulus is 2.0 × 1011 Pa, Poisson's ratio is 0.3, and density is 7850 kg/m^3. The water area is set around the geometric model. The water area parameters are as follows: the density is 1000 kg/m^3, and the speed of sound propagation in the water is 1500m/s.
3) Set physical field. The physical field is set to the acoustic-solid coupling type. Set the water area as pressure acoustic-boundary element. Add a background pressure field, the pressure field type is plane wave. The module for setting the geometric model is solid mechanics, and the displacement field and velocity field are initially set to zero values.
4) Meshing. Normally, when meshing, the maximum element size on the surface of the cylinder should theoretically be less than one-sixth of the acoustic wavelength.
5) Finite element solution. Under the premise that the above procedures are all set, set the frequency range to be sought, and then solve to obtain the scattered sound pressure data.

A. EXTRACTING THE POLES OF UNDERWATER SPHERICAL SHELL

For the above-mentioned underwater spherical shell, the COMSOL software was used to calculate the sound field scattering data of a total of 600 equally spaced frequency points in the 40-24000Hz frequency band. The sampling frequency is 48000Hz. The transmitted signal frequency in the experiment is 1500-24000Hz, covering the resonance area of the target [36], and the signal pulse width is 5ms.

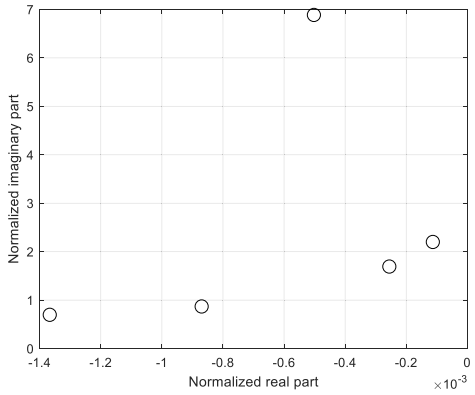

FIGURE 21. Distribution of the main poles of the underwater spherical shell.

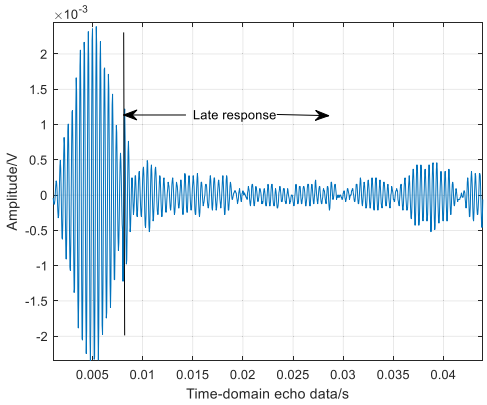

FIGURE 22. Time domain echo data of the underwater spherical shell.

Fig. 19 shows the sonar scattering cross-section data obtained by simulation.

Fig. 20 depicts the time-domain echo response signal.

A total of 400 points in the late time domain of the simulation were taken. Using the method of main pole extraction, the main pole distribution of the underwater spherical shell is shown in Fig. 21.

The spherical shell scattering data collected in the experiment is processed by filtering and energy accumulation (averaging the 10 echoes of the target). The time-domain echo data is shown in Fig. 22.

The first 5ms of Fig. 22 are the early echoes of the target, followed by the late time-domain echoes. The first 400 points of the late echoes are taken as input data for pole extraction. The main poles of the underwater spherical shell are shown in Fig. 23.

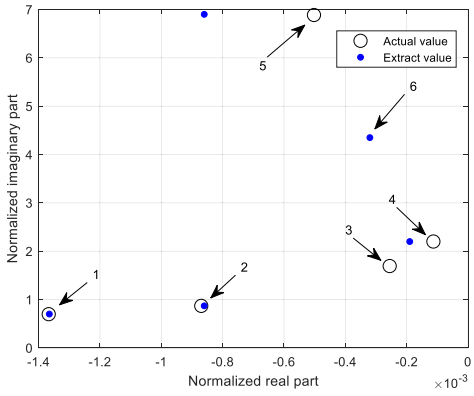

FIGURE 23. Experimental pole distribution of the underwater spherical shell.

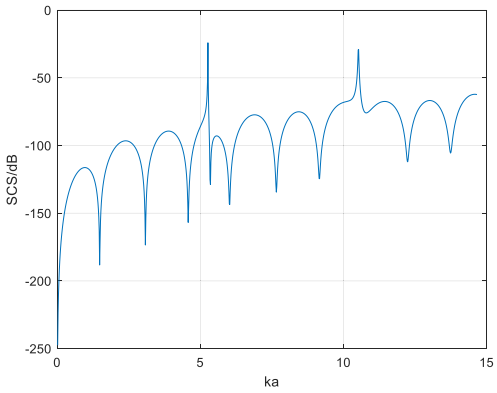

FIGURE 24. Sonar scattering cross section of the underwater thin rod.

It can be seen from Fig. 23 that two of the poles "1" and "2" extracted from the experimental data agree well with the actual poles. This is because the relative energy of the pole "1" is the largest, and the relative energy of the pole "2" is the second, and it is not easily affected by environmental factors. The pole "3" was not successfully extracted, because the relative energy of the pole is too small. The values of the poles "4" and "5" are significantly different from the estimated poles, and there are two possible reasons for the inaccurate extraction of the two poles or the extraction: (1) The relative energy of these two poles is not high, and they are easily interfered by environmental noise; (2) The slings and counterweights used in the experiment affected the vibration of the steel ball shell, causing the vibration of the steel ball shell to be excited. The final extracted poles were deviated from the actual values. An extra false pole "6" was extracted. This pole may be extracted as the main pole of the target because it was affected by auxiliary experimental equipment such as slings and counterweights.

B. EXTRACTING THE POLES OF UNDERWATER THIN ROD

For the above-mentioned underwater thin rod, the COMSOL software was used to calculate the sound field scattering data of a total of 1000 equally spaced frequency points in the 10Hz-10000Hz frequency band. The transmitted signal frequency in the experiment is 682-8000Hz, covering the resonance area of the target [36], and the signal pulse width is 5ms. The sampling frequency is 48000Hz. The simulated sonar scattering cross section is shown in Fig. 24.

The time domain echo response signal is shown in Fig. 25.

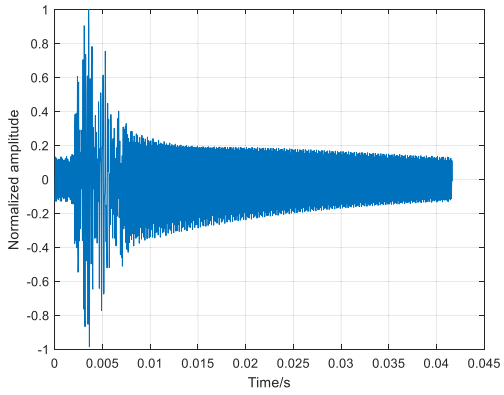

FIGURE 25. Time domain echo response of the underwater thin rod.

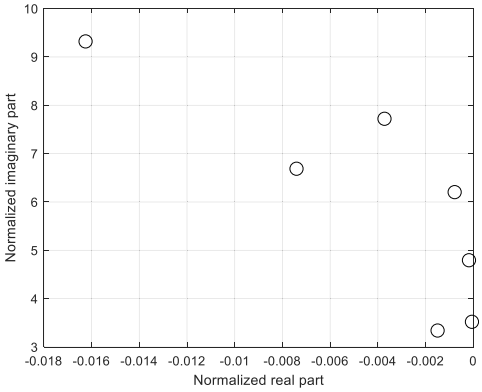

FIGURE 26. Distribution of main poles of the underwater thin rod.

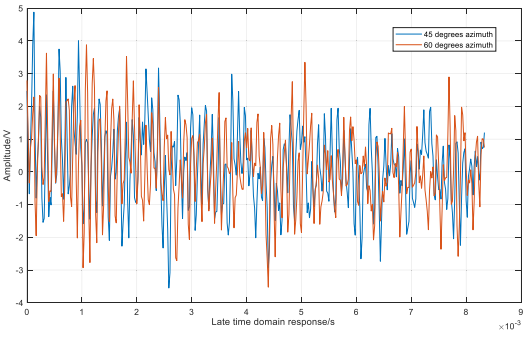

FIGURE 27. Time-domain late echo data of the underwater thin rod at incident angles of 45 and 60 degrees.

Using the method of extracting the main pole and integrating the multi-azimuth poles, the actual poles of the experimental thin rod obtained are shown in Fig. 26.

Fig. 27 is the late echo data obtained after the filtering of the underwater thin rod when the incident angles are 45 degrees and 60 degrees. The poles of the target have azimuth invariance. It can be seen from the figure that the attenuation trends of the late-time echoes in the two azimuths are approximately the same, and the frequencies are also approximately the same.

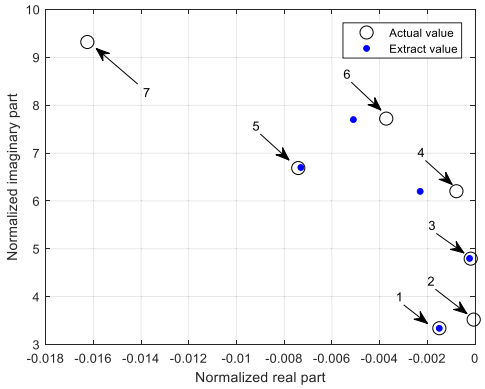

FIGURE 28. Pole distribution after integration of multiple azimuth poles on the underwater thin rod.

The experimental emission signal is incident on the target from 7 directions. The 7 orientations refer to 0-90 degrees, and the step interval is 15 degrees. 0 degree is to extract from the abeam direction of the thin rod and 90 degrees is to extract from the endpoint direction of the thin rod. The pole-scattering data collected from the experiments is used to extract the main poles in various orientations after pole extraction processing. The pole distributions obtained after the multi-azimuth pole integration is shown in Fig. 28

All false poles are eliminated through the integration of multi-azimuth poles. Three poles are consistent with the theoretical poles. The values of the poles "4" and "6" are significantly different from the actual poles. The possible reason is that the relative energy of these two poles is small, and the small environmental noise can cause the position to shift. The pole "2" was not extracted from the integrated distribution of multi-azimuth poles, probably because the relative energy of the pole is too small. The pole "7" is not extracted from the integrated distribution of multi-azimuth poles, because the transmitted signal does not include the frequency, and the pole is not successfully excited.

The above experiment of underwater steel ball shell and underwater thin rod proved the validity and accuracy of the method. It also shows when signal-to-noise ratio of the experimental data is higher we can get the better performance of overall system.

IV. CONCLUSION

This paper mainly focuses on the study of pole extraction in underwater target detection, by setting a reasonable value range and averaging the gathered poles to form a pole for extraction, the automatic determination of the number of target poles can be achieved. Furthermore, we showed by setting reasonable thresholds to extract the poles with large energy, the main poles of the target can be selected effectively. In view of the lack of the main poles of the target in some directions or the problem of residual false poles, the main poles in multiple directions of the target are integrated to obtain the final pole of the target. Finally, the field test results verified

that the pole extraction relying on matrix pencil method has well results in terms of underwater target detection.

REFERENCES

[1] M. Van Blaricum and R. Mittra, "Problems and solutions associated with Prony's method for processing transient data," *IEEE Trans. Electromagn. Compat.*, vol. EMC-20, no. 1, pp. 174–182, Feb. 1978.
[2] C. W. Chuang and D. L. Moffatt, "Natural resonances of radar targets via Prony's method and target discrimination," *IEEE Trans. Aerosp. Electron. Syst.*, vol. AES-12, no. 5, pp. 583–589, Sep. 1976.
[3] J. N. Brittingham, E. K. Miller, and J. L. Willows, "Pole extraction from real-frequency information," *Proc. IEEE*, vol. 68, no. 2, pp. 263–273, Feb. 1980.
[4] R. Kumaresan and D. Tufts, "Estimating the parameters of exponentially damped sinusoids and pole-zero modeling in noise," *IEEE Trans. Acoust., Speech, Signal Process.*, vol. 30, no. 6, pp. 833–840, Dec. 1982.
[5] M. D. Rahman and K.-B. Yu, "Total least squares approach for frequency estimation using linear prediction," *IEEE Trans. Acoust., Speech, Signal Process.*, vol. 35, no. 10, pp. 1440–1454, Oct. 1987.
[6] V. Jain, "Filter analysis by use of pencil of functions: Part I," *IEEE Trans. Circuits Syst.*, vol. CAS-21, no. 5, pp. 574–579, Sep. 1974.
[7] V. Jain, T. Sarkar, and D. Weiner, "Rational modeling by pencil-of-functions method," *IEEE Trans. Acoust., Speech, Signal Process.*, vol. ASSP-31, no. 3, pp. 564–573, Jun. 1983.
[8] Y. Hua and T. K. Sarkar, "Matrix pencil method for estimating parameters of exponentially damped/undamped sinusoids in noise," *IEEE Trans. Acoust., Speech, Signal Process.*, vol. 38, no. 5, pp. 814–824, May 1990.
[9] B. D. Rao, "Relationship between matrix pencil and state space based harmonic retrieval methods," *IEEE Trans. Acoust., Speech, Signal Process.*, vol. 38, no. 1, pp. 177–179, Jan. 1990.
[10] T. K. Sarkar and O. Pereira, "Using the matrix pencil method to estimate the parameters of a sum of complex exponentials," *IEEE Antennas Propag. Mag.*, vol. 37, no. 1, pp. 48–55, Feb. 1995.
[11] S. Ge, "Pole extraction of radar target echo based on improved matrix pencil algorithm," *Int. Electron. Elements*, vol. 26, no. 13, pp. 86–89, 2018.
[12] J. Chauveau, N. de Beaucoudrey, and J. Saillard, "Determination of resonance poles of radar targets in narrow frequency bands," in *Proc. Eur. Radar Conf.*, Oct. 2007, pp. 122–125.
[13] W. C. Chen and N. Shuley, "Utilizing the energy of each of the extracted poles to identify the dominant complex natural resonances of the radar target," in *Proc. IEEE Antennas Propag. Soc. Int. Symp.*, Jun. 2007, pp. 69–72.
[14] J. Chauveau, N. de Beaucoudrey, and J. Saillard, "Characterization of radar targets in resonance domain with a reduced number of natural poles," in *Proc. Eur. Radar Conf. (EURAD)*, 2005, pp. 69–72.
[15] J. Chauveau, N. de Beaucoudrey, and J. Saillard, "Resonance behavior of radar targets with aperture: Example of an open rectangular cavity," *IEEE Trans. Antennas Propag.*, vol. 58, no. 6, pp. 2060–2068, Jun. 2010.
[16] J. Chauveau, N. de Beaucoudrey, and J. Saillard, "Modification of resonance poles of a conducting target by a dielectric coating," in *Proc. Eur. Radar Conf.*, Oct. 2007, pp. 1719–1722.
[17] D. Moffatt and R. Mains, "Detection and discrimination of radar targets," *IEEE Trans. Antennas Propag.*, vol. AP-23, no. 3, pp. 358–367, May 1975.
[18] A. Berni, "Target identification by natural resonance estimation," *IEEE Trans. Aerosp. Electron. Syst.*, vol. AES-11, no. 2, pp. 147–154, Mar. 1975.
[19] E. Rothwell, D. Nyquist, K.-M. Chen, and B. Drachman, "Radar target discrimination using the extinction-pulse technique," *IEEE Trans. Antennas Propag.*, vol. AP-33, no. 9, pp. 929–937, Sep. 1985.
[20] D. Blanco, D. P. Ruiz, E. Alameda, and M. C. Carrion, "An asymptotically unbiased E-Pulse-Based scheme for radar target discrimination," *IEEE Trans. Antennas Propag.*, vol. 52, no. 5, pp. 1348–1350, May 2004.
[21] C. E. Baum, E. J. Rothwell, K.-M. Chen, and D. P. Nyquist, "The singularity expansion method and its application to target identification," *Proc. IEEE*, vol. 79, no. 10, pp. 1481–1492, Oct. 1991.
[22] G. Wu, W. Deng, Y. Jin, S. Yang, and T. Wang, "Radar target poles extraction based on the damping least squares algorithm," in *Proc. Congr. Image Signal Process.*, 2008.
[23] S. Yang, W. Deng, Q. Yang, G. Wu, and Y. Suo, "A frequency selection method based on the pole characteristics," *Int. J. Antennas Propag.*, vol. 2013, pp. 1–8, Jul. 2013.
[24] X. Yanran, J. Xin, and Z. Hongzhong, "Research Status of Pole Extraction Algorithms," *Chin. J. Ordnance Equip. Eng.*, vol. 39, no. 8, pp. 113–116, 2018.
[25] X. Ma, T. Wang, Y. Lin, and S. Jin, "Parallel iterative inter-carrier interference cancellation in underwater acoustic orthogonal frequency division multiplexing," *Wireless Pers. Commun.*, vol. 102, no. 2, pp. 1603–1616, Sep. 2018.
[26] M. Bailin, "A survey of singularity expansion methods," *Acta Electronica Sinica*, pp. 108–115, 1985.
[27] W. Xianliang, J. Dan, and W. Liangzhi, "Spline fitting and rational approximation methods for extracting poles from target transient response," *J. Univ. Sci. Technol. China.*, vol. 26, no. 4, pp. 528–533, 1996.
[28] X. Ma, B. Wang, L. Li, T. Wang, P. Hu, and Y. Lin, "A communication method between high-speed UUV and distributed intelligent nodes," *Mobile Netw. Appl.*, Oct. 2019.
[29] J. Dan, X. Shanjia, and W. Xianliang, "A new method for extracting natural frequency of target," *Prog. Natural Sci.*, pp. 65–71, 1999.
[30] Z. Zhaoben, H. Zengzheng, and W. Dezhao, "Pole method for recognizing underwater targets," *Acta Phys. Sinica*, pp. 538–546, 1984.
[31] L. Bosheng, "Extreme extraction of sonar target echo signal," *Acta Acoust.*, pp. 93–103, 1992.
[32] L. Bosheng, "Research on target transient pole extraction," *J. Harbin Inst. Shipbuilding Eng.*, no. 1, pp. 27–39, 1989.
[33] G. Qiao, X. Qing, W. Feng, S. Liu, D. Nie, and Y. Zhang, "Elastic feature of cylindrical shells extraction in time-frequency domain using biomimetic dolphin click," *J. Acoust. Soc. Amer.*, vol. 142, no. 6, pp. 3787–3795, Dec. 2017.
[34] G. Qiao, X. Qing, D. Nie, S. Ma, Y. Zhang, and J. Tang, "Underwater cylindrical shell in different thickness recognition using biomimetic dolphin clicks," in *Proc. OCEANS MTS/IEEE Monterey*, Sep. 2016, pp. 1–6.
[35] Y. Hua and T. K. Sarkar, "Matrix pencil and system poles," *Signal Process.*, vol. 21, no. 2, pp. 195–198, Oct. 1990.
[36] R. Toribio, J. Saillard, and P. Pouliguen, "Identification of radar targets in resonance zone: E-pulse techniques," *J. Electromagn. Waves Appl.*, vol. 17, no. 12, pp. 1723–1725, 2003.

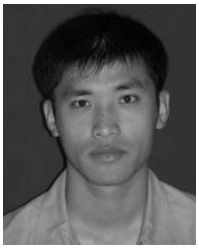

XUEFEI MA received the B.S. degree in electronic information engineering and the M.S. degree in information and communication engineering from Harbin Engineering University, China, in 2003 and 2006, respectively, and the Ph.D. degree in signal and information processing engineering from the School of College of Underwater Acoustic Engineering, Harbin Engineering University, in 2011. He is currently an Associate Professor with Harbin Engineering University. His research interests include the underwater acoustic detection, underwater acoustic communications, and underwater acoustic confrontation.

ZIQI ZHOU received the B.S. degree in communication engineering from Southwest Minzu University, China, in 2019. He is currently pursuing the M.S. degree with the School of College of Underwater Acoustic Engineering, Harbin Engineering University, China. His research interests include the underwater acoustic detection and the underwater acoustic communications.

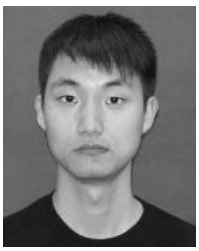

KAIYANG LIU received the B.S. degree in electronic information science and technology from the Hubei University of Education, China, in 2017. He is currently pursuing the M.S. degree with the School of College of Underwater Acoustic Engineering, Harbin Engineering University, China. His research interests include using underwater acoustic to detect small targets and the underwater acoustic field.

JIARONG ZHANG (Senior Member, IEEE) received the B.S., M.S., and Ph.D. degrees from Harbin Engineering University, China, He is currently a Senior Engineer with the Systems Engineering Research Institute. His current research interests include system engineering, underwater signal processing, and cross-medium communications.

WALEED RAZA received the B.E. degree in electronic engineering from the Department of Electronic Engineering, Dawood University of Engineering and Technology Karachi, Pakistan, in 2017. He is currently pursuing the M.S. degree in hydroacoustic engineering with the College of Underwater Acoustic Engineering, Harbin Engineering University, China. His research interests include underwater acoustic communications.